Tea eggs-inspired high-strength natural polymer hydrogels

Tengling Wu, Chunyan Cui, Chuanchuan Fan, Ziyang Xu, Yang Liu, Wenguang Liu [*]

School of Materials Science and Engineering, Tianjin Key Laboratory of Composite and Functional Materials, Tianjin University, Tianjin, 300350, China

ABSTRACT

Natural polymer (NP) hydrogels are an irreplaceable class of biomaterials owing to their identified biosafety; however, the intrinsic poor mechanical strengths severely limit their applications as structural tissue engineering scaffolds. Inspired by the stiffening albumen gel of tea eggs, a traditional Chinese snack, high-strength NP hydrogels are constructed by simply soaking in aqueous solution of tea polyphenols (TP), an active ingredient extracted from tea. The TP-treated representative NP hydrogels exhibit considerably enhanced multifaceted mechanical properties with maximum 19-/30-, 8.4-, 6.1-, 72-fold increases in tensile/compressive strengths, Young's modulus, elongation at break and facture toughness, respectively, compared with pristine hydrogels, primarily due to the hydrogen bonding interactions between TP and NP chains. The TP-treated NP hydrogels can resist different large deformations, which cannot be achieved by their original species at all. In aqueous solution, the TP-treated NP hydrogels can still maintain robust mechanical performances, in spite of somewhat decline in strengths with release of TP, which just favorably affords increased water contents, antibacterial and antioxidant activities. GelMA-TP hydrogel is shown to facilitate wound healing in a full-thickness skin defect model. Importantly, the weak 3D printed GelMA scaffolds are significantly strengthened by TP treatment, broadening the possibility for customizing individualized bioscaffolds.

1. Introduction

Natural polymer (NP) hydrogels are an important class of bio-materials in biomedical field due to its recognized biocompatibility and biodegradability [1,2]. However, conventional NP hydrogels are intrinsically limited by weak mechanical properties and a single function, severely limiting their applications as structural tissue engineering scaffolds [3–5]. Past decade has seen an enormous development of high-strength hydrogels in design principles [6,7]; however, previous studies are predominantly focused on synthetic polymer hydrogels [8–11]. Although much effort has been devoted to improving the mechanical strengths of natural polymer hydrogels, the strategies are mostly dependent upon introducing synthetic polymers, which unavoidably influences their biodegradability and biocompatibility [12]. Essentially, NPs are hydrophilic macromolecules, and high water affinity tends to break intermolecular hydrogen bonds even if the network is chemically crosslinked due to the competition of water with inter-polymer hydrogen bonds. Surveying literature reveals that the weak mechanical properties of NP hydrogels reported thus far are originated from lacking of built-in water-shielding mechanism. Whereas

the intrinsic hydrogen bonds in original macromolecular chains are too weak to resist water attack.

As we know, tea eggs is one of the famous snacks in China. A common sense is that ordinary heat-induced albumen gel is fragile and weak, but the strength of the albumen gel of tea-marinated eggs is significantly enhanced, which is speculated to stem from enhanced network density caused by the hydrogen bonding interactions between the active substances in tea and albumen [13–15]. An idea popping into mind is that whether soaking in tea water could contribute to an increased mechanical strength of natural polymer hydrogels. To test this idea, methacrylated gelatin (GelMA) hydrogel and agarose (AG) hydrogel that are frequently used in tissue engineering field were selected to be immersed in West Lake Longjing tea water for 24 h. We can judge that the tensile strength of tea water-treated GelMA hydrogel is enhanced from original 0.05 MPa to 0.32 MPa, and the elongation at break is increased from original 55% to 124% (Fig. 1). Similarly, tea water-treated AG hydrogel also exhibits an improved mechanical strength with tensile strength increasing from original 0.12 MPa to 0.31 MPa, and the elongation at break increasing from 26% to 44% (Fig. 1). The initial results reveal that tea water treatment can lead to an

---

enhancement in mechanical performance of both GelMA and AG hydrogels to a different extent. Nonetheless, this improvement is not prominent possibly due to diluted active constituents in tea water. Previous analytic test has identified that tea polyphenols (TP) is a group of polyphenol compounds extracted from tea (the chemical structures are illustrated in Fig. 1 and Fig. S1) [16,17]. As a kind of polyphenols, tannic acid (TA) has been reportedly used to enhance the mechanical strength of hydrogels, and the reinforcing mechanism was supposed to stem from hydrogen bonding interaction between phenols and polymers. For instance, soaking GelMA hydrogel into TA solution could lead to increased tensile strength and elongation at break, respectively, compared with the pristine GelMA hydrogel [18]. Several studies also revealed that soaking polyvinyl alcohol or polyacrylamide hydrogels into TA solution could enhance the mechanical performances of parent hydrogels [19]. Nevertheless, previous studies have identified that the concentrated TA may have injurious effects upon the liver [20,21]. While TP has been proved to have anti-oxidation, wound-healing, anti-bacterial functions [22–26]. Our initial experimental results revealed that TP-treated egg white gel exhibited an 8-fold enhancement in compressive strength compared to original egg white gel (Fig. S2). Thus far, we hypothesize that treating different natural polymer hydrogels with TP may afford a simplified and universal approach to generate a variety of biomacromolecule-based high-strength antibacterial and antioxidant hydrogels. To testify our hypothesis, we designed a series of experiments, as shown in Fig. 1.

2. Experimental section

2.1. Materials

Gelatin (Type A from porcine, 300 g bloom, Sigma-Aldrich, USA), methacrylic anhydride (98%, Sigma-Aldrich, USA), 2-hydroxy-2-methyl-1-phenyl-1-propanone (IRGACURE 1173, 98%, Sigma-Aldrich, USA), agarose (Electrophoretic grade, 750 g cm^{-2}, Yuanye, China), sodium alginate (low viscosity, Sigma-Aldrich, USA) green tea polyphenols (TP, 98%, ENERGY, China), tannic acid (Aladdin, China), calcium chloride (Kermel, China), sodium hydroxide (Kermel, China), and urea (Kermel, China), were used as received. All the other reagents are of analytical grade and used without further purification.

2.2. Synthesize of methacrylated gelatin (GelMA)

4 g of gelatin was dissolved in 200 mL deionized water at 40 °C and then 132 mL DMF was added until the solution was clarified. Subsequently, methacrylic anhydride was added and the reaction proceeded at 40 °C for 2 h. The mixture was precipitated with ethanol, and then dissolved in deionized water and lyophilized to obtain the resultant GelMA.

2.3. Preparation of GelMA hydrogels, GelMA-TP hydrogels, and GelMA-TA hydrogels

The GelMA hydrogels were synthesized by photoinitiated radical polymerization. First, a GelMA solution with a mass fraction of 20% was prepared by dissolving lyophilized foam in distilled and deionized water, followed by addition of 1173 (2 wt% relative to the total monomer content) with vigorous stirring. The resulted solution was injected into a transparent plastic rectangular mold or a cylindrical mold, and polymerization was performed for 40 min in a UV cross-link oven (365 nm, XL-1000 UV Cross-linker, Spectronics Corporation, NY, USA) to obtain GelMA hydrogels. The obtained GelMA hydrogels were immersed in TP or TA solutions at 37 °C to obtain GelMA-TP or GelMA-TA hydrogels.

2.4. Preparation of agarose (AG) hydrogels and AG-TP hydrogels

AG hydrogels were easily formed by casting AG solution (3% m/v) into mold and then cooling to ambient temperature. The obtained AG hydrogels were immersed in TP solutions at 37 °C to obtain AG-TP hydrogels.

2.5. Synthesize of methacrylated alginate (AlgMA)

AlgMA was synthesized referring to a previous report [27]. 2 g of alginate was dissolved in 100 mL 0.2 mol L^{-1} NaOH solution, followed by addition of 20 mL methacrylic anhydride, and the reaction proceeded for 24 h. The mixture was precipitated with acetone, and then dried to obtain the resultant AlgMA.

2.6. Preparation of AlgMA-Ca^{2+} and AlgMA-Ca^{2+}-TP hydrogels

The AlgMA hydrogels were synthesized by photoinitiated radical polymerization. First, an AlgMA solution with a mass fraction of 8% was prepared by dissolving AlgMA in distilled and deionized water, followed by addition of 1173 initiator (2 wt% relative to the total monomer content) with vigorous stirring. Then, the solution was injected into a transparent plastic rectangular mold, and polymerization was performed for 40 min in a UV cross-link oven (365 nm, XL-1000 UV Cross-linker, Spectronics Corporation, NY, USA) to obtain AlgMA hydrogels, which was immersed in 0.5 mol L^{-1} calcium chloride solution for 1 h. The obtained AlgMA-Ca^{2+} hydrogel were immersed in TP (20%) solutions to obtain AlgMA-Ca^{2+}-TP hydrogels.
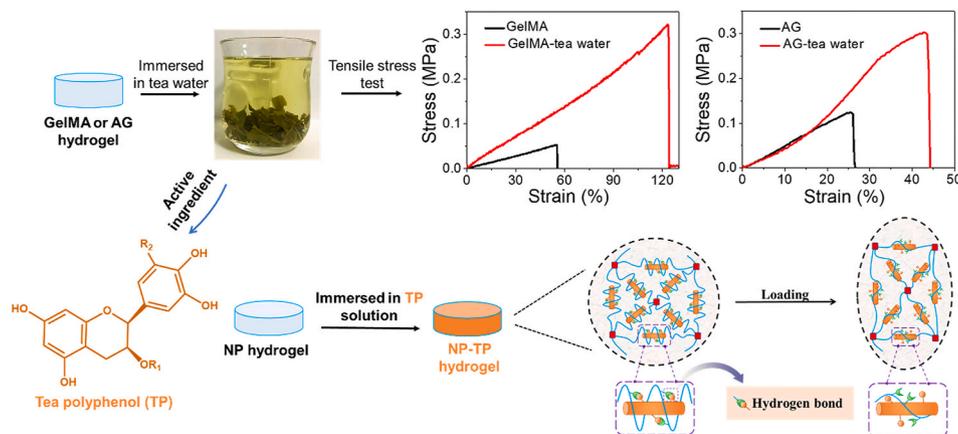
Fig. 1. Tea water-induced the increased mechanical strengths of GelMA and AG hydrogel; schematic illustration of the formation of NP-TP hydrogel and toughening mechanism.

2.7. Characterizations

Fourier transform infrared (FTIR) spectrometry (Nicolet 6700, USA) was used to characterize the formation of the hydrogels. The morphology and microstructure of the hydrogel were investigated by using a field-emission SEM (FEI Quanta S-4800 FE-SEM).

2.8. Water content measurements

The moisture on the surface of the hydrogel was wiped off and the wet weight (m_{wet}) was recorded on an analytical balance. Then the hydrogel was left to dry in a 60 °C vacuum oven until the weights were constant (m_{dry}). The water content of the hydrogels is defined as: Water Content = $(m_{wet} - m_{dry})/m_{wet} \times 100\%$.

2.9. Measurement of mechanical properties

The mechanical properties of the hydrogels were tested on Instron 2344 Microtester at room temperature. For tensile test, the crosshead speed was set at 50 mm min^{-1}. For compression test, the compression rate was set at 10 mm min^{-1}. At least three specimens were used for each mechanical test.

2.10. Measurement of in vitro TP release

The GelMA-TP hydrogel discs with a diameter of 10 mm and a thickness of 0.5 mm were placed in 8 mL PBS at 37 °C. At predetermined periods, 0.5 mL of buffer solutions was collected and replaced with an equal amount of PBS and its absorbance at 274 nm was measured by UV–visible spectrophotometer (TU-1810 UV–vis spectrophotometer).

2.11. 3D printing

Hydrogel constructs were fabricated by a 3D bioprinter (3D Bio-Architect® Sparrow Regenovo Biotechnology, Hangzhou, China) with a low-temperature deposition platform. The CAD/CAM software were used to build up the designed 3D architectures. Subsequently, the GelMA/Alg mixture (15% GelMA solution and 3% Alg solution were mixed by equal volume) was firstly loaded into the syringe and maintained at 30 °C for 5 min. Then, the GelMA/Alg mixture was extruded through the needle (air pressure was set as 0.07 MPa) and printed directly on the refrigerated platform (10 °C). Finally, the 3D printed objects were polymerized to solidify and stabilize the structures under UV irradiation for 40 min.

2.12. Antioxidant activity

The antioxidant activity of the GelMA-TP hydrogel was evaluated through 1,1-diphenyl-2-picrylhydrazyl (DPPH) assay. Briefly, 2.5 mg GelMA-TP hydrogel was immersed in 25 mL of DPPH solution (0.1 mmol L^{-1}, in 80 wt% methanol) in dark, and the absorbance of the mixture solution at 520 nm was measured at every 5 min interval and the scavenging on DPPH radicals was assessed by the following formula: ROS clearance (%) = $(AB - AS)/AB \times 100\%$, where AB is the absorbance of control (DPPH only) and AS is the absorbance of the sample (DPPH + sample).

2.13. In vitro antibacterial capability of hydrogels

The antibacterial activity of GelMA-TP hydrogel against *S. aureus* (Gram-positive bacteria) and *E. coli* (Gram-negative bacteria) was evaluated through inhibition zone method and flat colony counting method. For inhibition zone method, 200 μL bacterial suspension of *E. coli* or *S. aureus* (10^6 CFU mL^{-1}) was spread in solid culture media (LB medium with 1% agar) dish, and then the GelMA hydrogels or GelMA-TP hydrogels were gently placed upon the solid medium. The solid

culture media in the absence of bacterial was set as blank group and the untreated was set as control group. The culture dishes were incubated at 37 °C for 24 h, and the zone of inhibition was observed. For flat colony counting method, 400 μL bacterial suspension of *E. coli* (10^5 CFU mL^{-1}) or 400 μL bacterial suspension of *S. aureus* (10^5 CFU mL^{-1}) was cultivated respectively with GelMA hydrogel and GelMA-TP hydrogel, and the untreated bacterial suspension was set as control group. After 6 h cultivation, 200 μL of the above suspensions were spread in solid culture media. Subsequently, the culture dishes were incubated at 37 °C for 24 h with the following observation and photographing of bacteria growth.

2.14. Cell viability assay in vitro

The cytotoxicity of the GelMA-TP hydrogel was evaluated using the reported co-culture method [28].

2.15. In vivo degradation test

All of the protocols for animal experiments were carried out according to the guidelines of the Council for the Purpose of Control and Supervision of Experiments on Animals, Ministry of Public Health, China, and approved by Animal Ethics and Welfare Committee of Institute of Radiation Medicine, Chinese Academy of Medical Sciences (DWLL-2020104). The in vivo degradation of the GelMA-TP hydrogel was evaluated according to our previous method [29].

2.16. In vivo wound healing assay

A full-thickness skin defect wound model was created to evaluate the activity of the GelMA-TP hydrogel in facilitating wound healing. All the hydrogels were sterilized through autoclaving prior to the experiment. 21 SD (weight 230 g) rats were randomly divided into three groups. First, a defect with a diameter of 10 mm was constructed on the dorsal skin of the mouse, and then the wounds were respectively treated by GelMA hydrogel, GelMA-TP hydrogel. The untreated skin defects served as the control group. The hydrogels were replaced every 3 days and the change of wound was photographed. The wound area was calculated using Image J software and the wound closure rate was obtained according to $(S_0 - S_t)/S_0 \times 100\%$, where S_0 is the original wound area and S_t is the wound area at a specific time point. The animals were euthanized at 12 days and the skin tissue samples were fixed with 4% paraformaldehyde for hematoxylin and eosin (H&E) staining.

2.17. Statistical analysis

Data are presented as means ± standard deviations. ANOVA was used to determine whether data groups differed significantly from each other. Statistical significance was defined as having *P < 0.05.

3. Results and discussion

3.1. Preparation and characterizations of GelMA and GelMA-TP hydrogels

First, the GelMA was synthesized according to our previous study and the degree of methacrylation was determined to be 66% by ^{1}H NMR spectra [30]. Then the GelMA (20% m/v) hydrogel formed by free radical photopolymerization was selected in the following experiment. The GelMA-TP hydrogels were obtained through immersing the GelMA hydrogel into TP solutions, and the basic chemical structure of different hydrogels was confirmed by Fourier transform infrared (FT-IR) spectra. As shown in Fig. S3, the peak at 3384 cm^{-1} of TP is attributed to the symmetrical stretching vibrations of the hydroxyl groups [31]; the peaks at 1642 and 1526 cm^{-1} from the GelMA hydrogel are attributed to the characteristic bands of the gelatin backbone, and the band at 3326 cm^{-1} is assigned to the N–H vibration in the GelMA hydrogel, which shifts to

3309 cm^{-1} in GelMA-TP hydrogel [32], suggesting the formation of hydrogen bonds between GelMA and TP.

3.2. Mechanical properties of the GelMA-TP hydrogels

The effects of TP on the mechanical performances of GelMA hydrogels were systematically evaluated. The GelMA hydrogels were immersed in TP solutions with different concentrations (10%, 15%, 20%) at 37 °C, and then their mechanical properties were measured after 6 h. As shown in Fig. 2A, the tensile stress of GelMA hydrogel is greatly enhanced after TP treatment. However, there is no significant difference in the mechanical properties of GelMA hydrogel treated with 20% TP and 15% TP solutions (Fig. 2B and C). Therefore, a 20% TP solution was chosen in the following experiment to test the influence of

immersion time on the mechanical properties of GelMA hydrogels, and the formed GelMA-TP hydrogels are termed as GelMA-TP-x (x donates the immersion time).

Fig. 2D and G exhibit that TP treatment contributes to a significant increase in mechanical properties of the GelMA hydrogel with time. The pristine GelMA hydrogel is ruptured easily at a small tensile stress (50 kPa)/strain (55%), and compressive stress (150 kPa)/strain (42%). In comparison, the GelMA-TP hydrogels demonstrate much higher mechanical performances with respectively 19-, 8.4-, and 5-fold increase in tensile strength (from 0.06 to 1.14 MPa), Young's modulus (from 0.09 MPa to 0.76 MPa), and fracture strain (from 55% to 276%) as the immersion time is increased from 0 to 48 h (Fig. 2E and F). Remarkably, the fracture toughness of GelMA-TP-48h hydrogel can reach 1.13 MJ m^{-3}, 72 times higher than that of the original GelMA hydrogel, indicating the
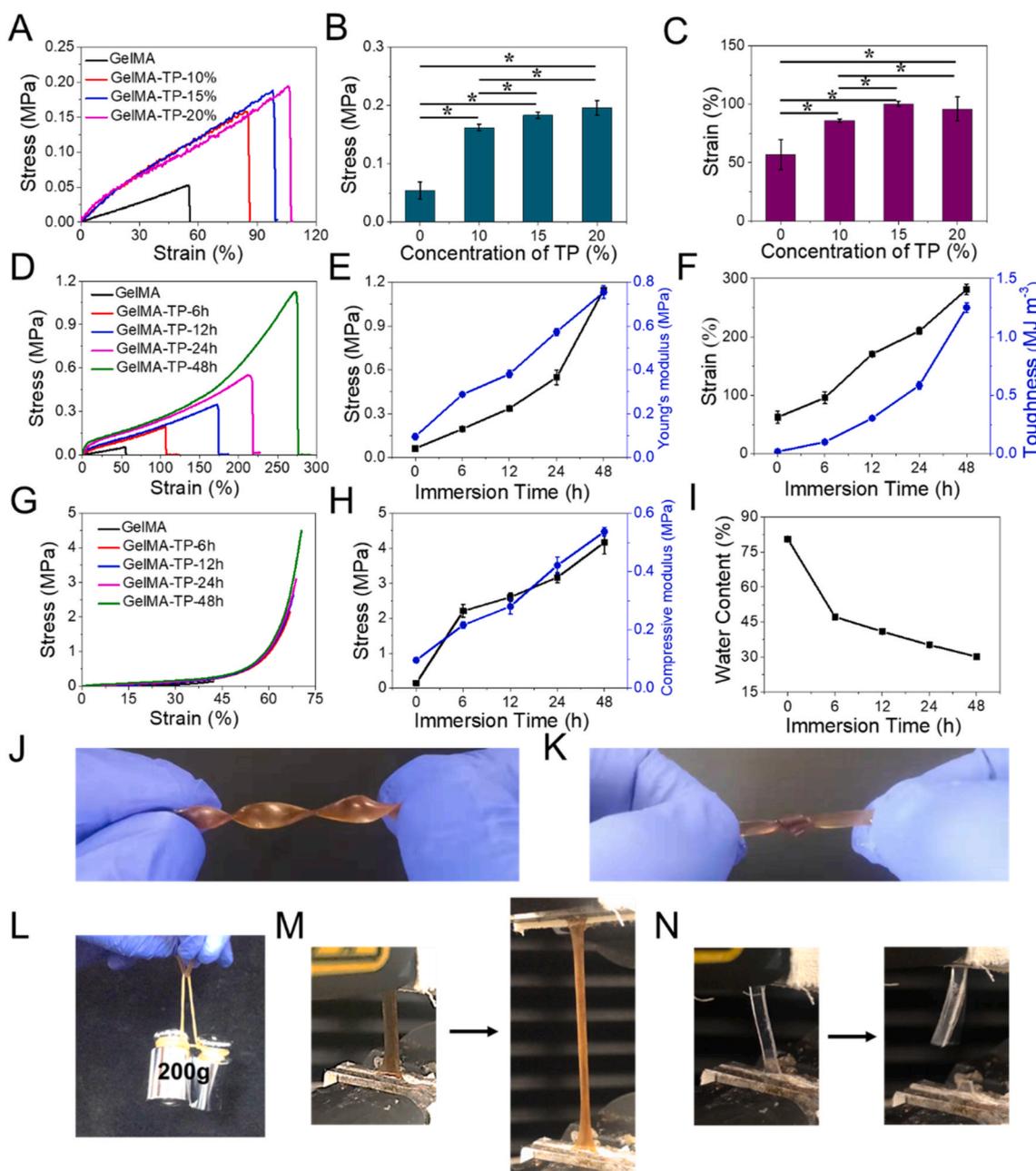
Fig. 2. A-C) Tensile performance of GelMA hydrogels treated with different concentrations of TP solutions. D-F) Tensile performance of GelMA-TP-x hydrogels. G-H) The compressive performance of GelMA-TP-x hydrogels. I) Water contents of GelMA-TP hydrogels. J) Digital images of the GelMA-TP hydrogel showing an ability to withstand twisting; K) knotting; L) 200 g weight loading and M) stretching. N) Digital images of GelMA hydrogel under stretching. (* indicates significance, *p < 0.05).

TP-induced high toughness. Likely, the compressive strength and modulus are enhanced from 0.15 MPa to 4.5 MPa, 0.09 MPa to 0.54 MPa, respectively, with increasing soaking time from 0 to 48 h (Fig. 2D and H). Macroscopically, the obtained GelMA-TP-48h hydrogel (as a representative example) can withstand twisting, knotting, heavy loading, and even stretching (Fig. 2J-M), while the pristine GelMA hydrogel is very brittle with almost no malleability (Fig. 2N). Thus far, we consider that the hydrogen bonding interactions between GelMA and TP resulted in a tremendous increase of mechanical properties.

Next, the water contents of GelMA-TP hydrogels were tested (Fig. 2I). The water content of the GelMA-TP hydrogels declines from 80% to 31% as the immersion time increases. The GelMA are more inclined to form hydrogen bonds with polyphenol than with water molecules. Therefore, during the soaking treatment, more hydrogen bonds are formed between polymer chains and TP, thereby leading to much denser network structure. The volume of the hydrogel is gradually reduced with time (Fig. S4), which is consistent with the changing trend of water contents. SEM tests were conducted to observe the changes in the hydrogel network structure. It is seen that the GelMA-TP hydrogel has a more compact network than GelMA hydrogel (Fig. S5).

Also, loading-unloading tests were performed to evaluate the energy dissipation of GelMA-TP hydrogels. Fig. 3A shows that under the same strain, the area of the hysteresis loop is considerably increased with the increase of TP immersion time, suggesting that more sacrificial bonds are formed. In the GelMA-TP network, the H-bonding interactions between GelMA and TP serve to dissipate external energy. The dissipated energy (U_{hys}) of original GelMA hydrogel that is calculated from the area between the loading-unloading curve is only 1.4 kJ m^{-3}, while the GelMA-TP-48h hydrogel can dissipate 58 kJ m^{-3} energy under 50% strain, which is 40-time higher than that of GelMA hydrogel, implying

that the hydrogen bonds between GelMA and TP results in a high toughness and strength (Fig. 3B).

To evaluate the stability of the GelMA-TP hydrogel in physiological environment, we determined the mechanical properties of the GelMA-TP hydrogel in PBS at 37 °C. Prior to mechanical test, we first measured the release TP in PBS at 37 °C. Fig. S6 shows that TP comes out rapidly at the beginning 12 h, and then is slowly released within 12–24 h. Eventually, the release levels off after 48 h. Subsequently, the mechanical properties of GelMA-TP-48h hydrogel immersed in PBS at 37 °C (replacing PBS every 12 h) for different time periods were measured. As shown in Fig. 3D, its mechanical properties decrease with the increase of soaking time. At the beginning 12 h, the strength exhibits a rapid downward trend, because a large amount of free TP diffuses out, and water molecule permeates into the network, leading to decreased hydrogen bonding interactions. Clearly, after soaking for 48 h, the mechanical properties become stable, which is consistent with the release curve of TP. After 72 h of soaking in PBS, the hydrogel can maintain the tensile strength, Young's modulus, elongation at break and toughness at 0.39 MPa, 0.36 MPa, and 200%, and 0.35 MJ m^{-3}, respectively (Fig. 3C–E). This indicates that the GelMA-TP hydrogel can maintain robust mechanical properties even if it is soaked in PBS at 37 °C for 72 h. The similar trend is also observed in the compressive test, where the compressive strength and modulus can be maintained at 1.03 MPa and 0.25 MPa at the ultimate test time (immersed in PBS for 72 h) (Fig. 3F and G). Notably, the water content of GelMA-TP-PBS-72h can bounce back to 55%. In order to further verify the hydrogen bonding interactions between TP and GelMA hydrogel, the GelMA-TP-48h hydrogel was immersed in 5 mol L^{-1} urea solution (a hydrogen bond breaking agent) and the mechanical test was carried out after 24 h. As shown in Fig. 3H, the tensile stress of the GelMA-TP-48h hydrogel after soaking in
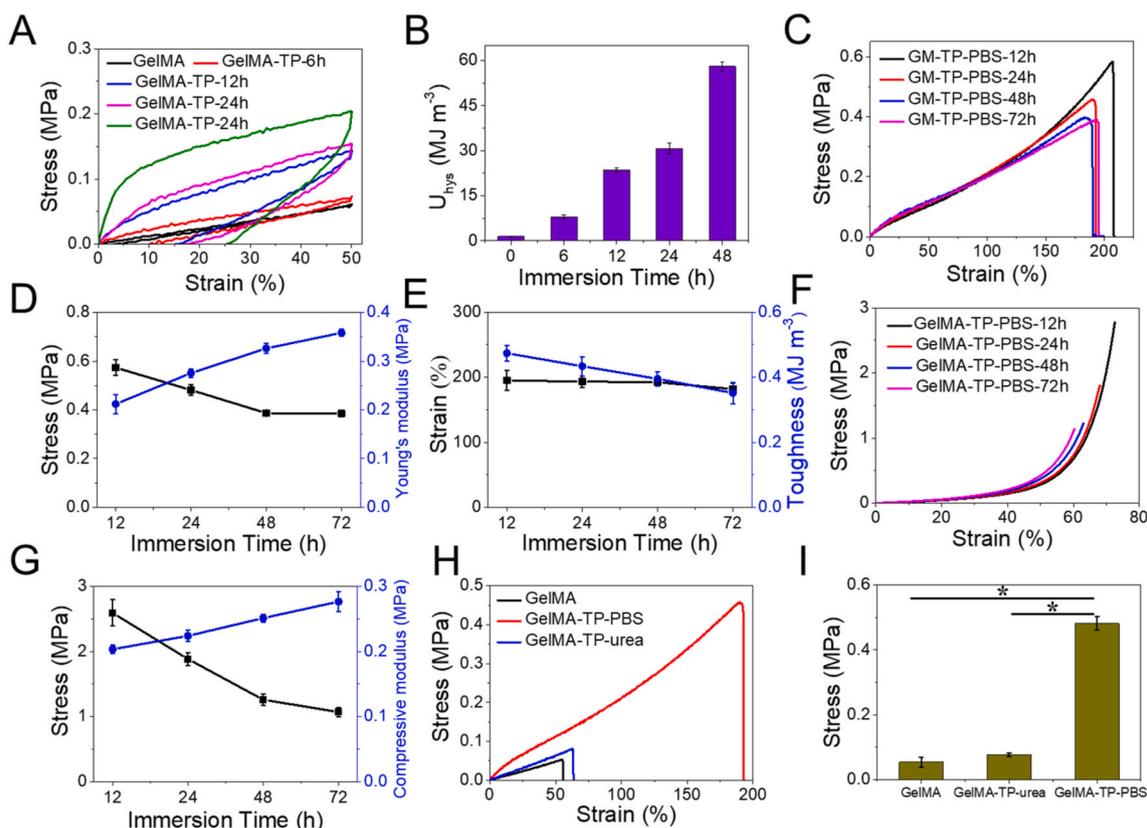
Fig. 3. A) Tensile loading–unloading curves of GelMA hydrogel and GelMA-TP-x hydrogels over a strain range of 0–50%. B) The calculated dissipated energy of GelMA hydrogel and GelMA-TP hydrogels under 50% strain. C-E) The variation in tensile performance of GelMA-TP-48h hydrogels with immersing time in PBS ranging from 12 to 72 h. F-G) The variation in compressive performance of GelMA-TP-48h hydrogels with immersing time in PBS ranging from 12 to 72 h. H) The tensile stress-strain curves and I) tensile stress of GelMA, GelMA-TP-PBS and GelMA-TP-urea hydrogels. (* indicates significance, *p < 0.05).

PBS for 24 h can reach 0.45 MPa, but after soaking in the urea solution the tensile strength drops sharply to 80 kPa, a significant loss, which is similar to the mechanical properties of pristine GelMA hydrogel (Fig. 3I). This suggests that urea leads to breakup of the hydrogen bonds between TP and polymer chains, indirectly proving that the enhancement mechanism of TP is primarily originated from hydrogen bonding interactions between TP with GelMA.

To highlight the uniqueness of TP in enhancing mechanical strengths of NP hydrogels, another polyphenol, tannic acid (TA) with a higher molecular weight was compared in parallel. In a similar way, the GelMA hydrogel was immersed in TA solution. Although the GelMA-TA hydrogel achieved enhanced mechanical strengths with increase of immersion time (Fig. S7), the mechanical strengths of the resultant GelMA-TA are much lower than those of GelMA-TP hydrogels. Of course, water content may affect the mechanical strengths. We note that after immersing in TA for 48 h, the water content of GelMA-TA-48h hydrogel was determined as 34%, similar to that of GelMA-TP-48h. Whereas the tensile strength, elongation at break, Young's modulus and toughness of the GelMA-TA hydrogels at 48 h post-immersion are measured to be 0.25 MPa, 141%, 0.57 MPa, 0.21 MJ m^{-3}, respectively. These results indicate that TP is more potent in enhancing the mechanical properties of GelMA hydrogel. A possible reason is that small molecular weight TP can diffuse more easily into the hydrogel to form more hydrogen bonds with GelMA, thus resulting in more significant enhancement of mechanical strengths. While the larger molecular skeleton may restrain the permeation of TA into the network; as a result, fewer hydrogen bonds are formed. To discriminate the H-bonds of TP and TA with GelMA, the GelMA-TP-48h and GelMA-TA-48h hydrogels were respectively placed into 5 mol L^{-1} urea solution for 1 h, and then their tensile strengths were tested. Fig. S8 shows that the tensile stress of GelMA-TA-48h hydrogel decreases to almost the same level as that of the pristine GelMA hydrogel; however, the GelMA-TP-48h can still withstand a 0.21 MPa of tensile strength, proving that the hydrogen bonding between TP and GelMA is stronger.

3.3. TP-strengthened AG hydrogels and AlgMA-Ca^{2+} hydrogels

To examine the universality of TP reinforcement, agarose (AG) hydrogel was formed by cooling down its aqueous solution (3% m/v) to room temperature. Then the AG hydrogel was treated with TP as above described. In FTIR spectra (Fig. S9), the peaks at 3384 cm^{-1} in TP and 3307 cm^{-1} in AG are attributed to the symmetrical stretching vibrations of the hydroxyl groups, respectively [33]. While in the AG-TP hydrogel, the peak is shifted to 3303 cm^{-1}, indicating the formation of hydrogen bonds between AG and TP. Analogously, TP can greatly enhance the mechanical properties of the AG hydrogel (Fig. 4A–D). The AG-TP hydrogel can be twisted, knotted and stretched. Comparatively, the pristine AG hydrogel is very weak and almost non-stretchable (Fig. 4E). Fig. 4F and G presents the test results of mechanical properties, where the tensile strength and elongation at break of the AG hydrogel are shown to reach 0.52 MPa and 153%, respectively, after soaking in TP for 6 h, which are 4.3-time and 7.2-time those of the AG hydrogel. We also measured their stability in PBS. As shown in Fig. 4H and I, the AG-TP hydrogel can maintain a tensile strength of 0.3 MPa and a breaking strain of 50% after 72 h of immersion in PBS, indicating a better mechanical stability in salt solution. Herein, the strengthening effect of TP on methacrylated alginate (AlgMA)-Ca^{2+} hydrogel was also tested. Fig. S10 presents the test results of mechanical properties, where the tensile strength, Young's modulus, elongation at break and toughness of the AlgMA-Ca^{2+}-TP hydrogel are shown to reach 1.68 MPa, 5.26 MPa, 280% and 2.63 MJ m^{-3}, respectively, after immersing in TP for 2 h, which are 3.9-time, 5.4-time, 2.2-time and 7.3-time those of the AlgMA-Ca^{2+} hydrogel.

3.4. TP-strengthened 3D printed hydrogels

Currently, 3D printing has been hailed as a transformative technology to customize tissue engineering scaffolds for individualized therapy. Nevertheless, lack of robust biocompatible inks has greatly limited its clinical application. To afford printability, alginate (Alg) was mixed with GelMA aqueous solution. The GelMA/Alg mixture exhibits an
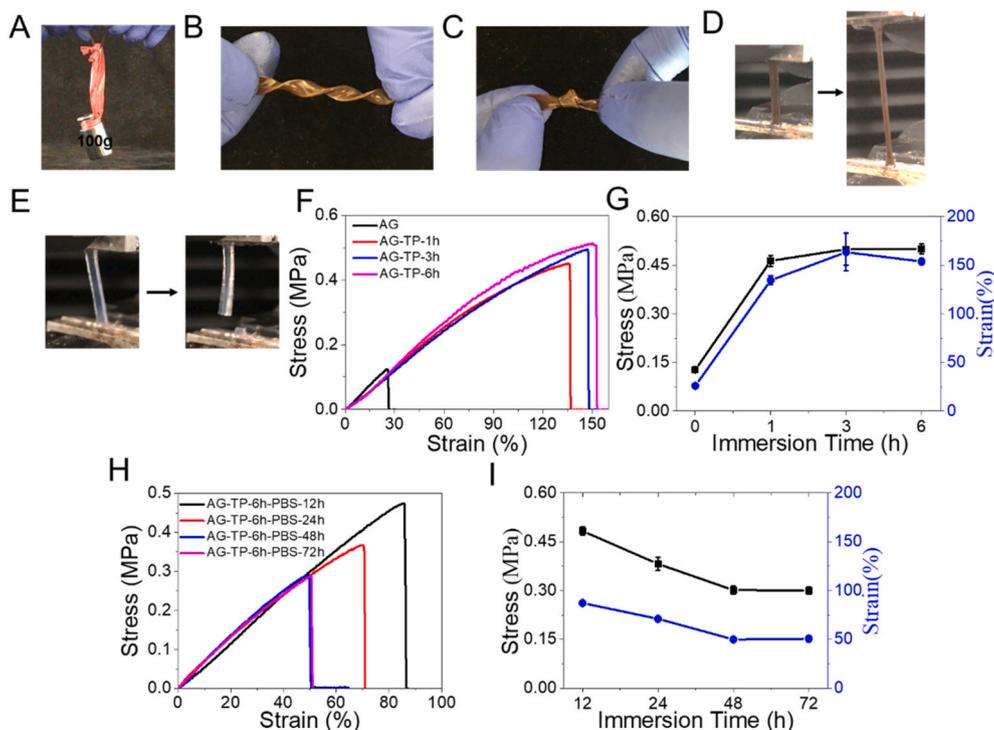
Fig. 4. Digital images showing an ability of the AG-TP hydrogel to lift a 100 g weight (A), withstand twisting (B), knotting (C) and stretching (D). Digital images showing the stretched AG hydrogel (E). Tensile performance of AG-TP-x hydrogels (F, G). Tensile performance of AG-TP-PBS hydrogels (H, I).

excellent printability (Video S1). Several representative hexagon (the side length is 2 cm), triangle (the length of the bottom edge is 4 cm) and square (the side length is 3 cm) objects are printed (Fig. 5A), which are polymerized to solidify and stabilize the structures. Then the printed objects are soaked in the TP solution for 12 h. Evidently, the TP-treated constructs are shrunken considerably and retain a high printing fidelity. In comparison, the side lengths of hexagon and square decreases to 1.4 and 2.1 cm, respectively; the length of the triangle's bottom edge is reduced to 2.8 cm (Fig. 5B). Fig. 5C displays that the TP-reinforced rectangular gel grid can resist bending, curling and even lift a 500 g weight (1000-time its own weight). On the contrary, the 3D printed hydrogel network without TP treatment can be easily broken. (Videos S2 and S3). The TP-treated GelMA/Alg hydrogel printed fishing net can bear a 100 g weight (Fig. 5D) and withstand the falling of a 100 g ball without damage (Video S4). Next, the tensile properties of 3D printed GelMA/Alg and GelMA/Alg-TP hydrogels were also measured. As shown in Fig. 5E, the tensile stress and elongation at break of 3D printed GelMA/Alg pristine hydrogel are only 0.12 MPa and 42%, respectively; while the GelMA/Alg-TP hydrogel becomes much stronger and elastic with a 0.72 MPa tensile strength and a 102% breaking strain.

Supplementary data related to this article can be found at https://doi .org/10.1016/j.bioactmat.2021.02.009.

3.5. In vitro antioxidant and antibacterial properties of GelMA-TP hydrogels

It has been established the TP has a function of scavenging free radicals [25,34]. Therefore, we studied the free radicals scavenging capacity of the GelMA-TP hydrogel through 1,1-diphenyl-2-picrylhydrazyl (DPPH) assay. 2.5 mg GelMA-TP-48h hydrogel was placed in 25 mL DPPH solution and photographed every 5 min. As illustrated at Fig. 6A, the DPPH solution changes from purple to yellow as time elapses, implying that the GelMA-TP hydrogel can effectively remove the DPPH radicals. In addition, we measured the absorbance at 520 nm and calculated the scavenging rate of DPPH radicals. The absorbance at 520 nm is shown to decrease with incubation time; the absorption peak at 520 nm almost disappears at 20 min and the ROS clearance rate can reach 67.5% at 15 min (Fig. 6B and C). This indicates that the GelMA-TP hydrogel has an excellent free radical scavenging activity. Then we evaluated the antibacterial activity of GelMA-TP hydrogel against *S. aureus* and *E. coli* in vitro. As illustrated in Fig. 6D, the GelMA-TP hydrogel exhibits an obvious antibacterial loop against *E. coli* (the
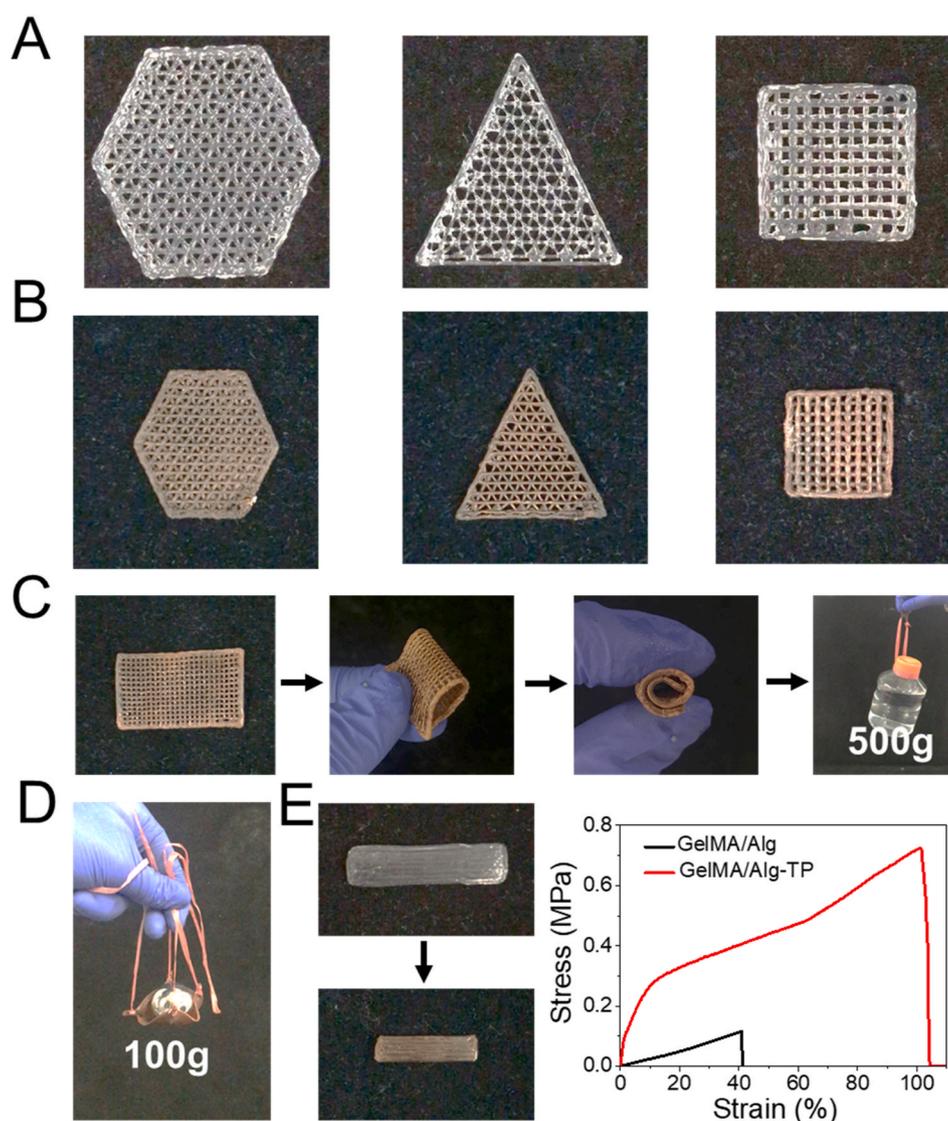
Fig. 5. A) Pictures of 3D printed hexagon, triangle and square hydrogels. B) The pictures of 3D printed hexagon, triangle and square hydrogels after TP treatment. C) TP-reinforced rectangular gel grid can resist bending, curling and a 500 g weight loading. D) TP-treated web structure hydrogel can hold a 100 g weight. E) The tensile properties of 3D printed hydrogels.
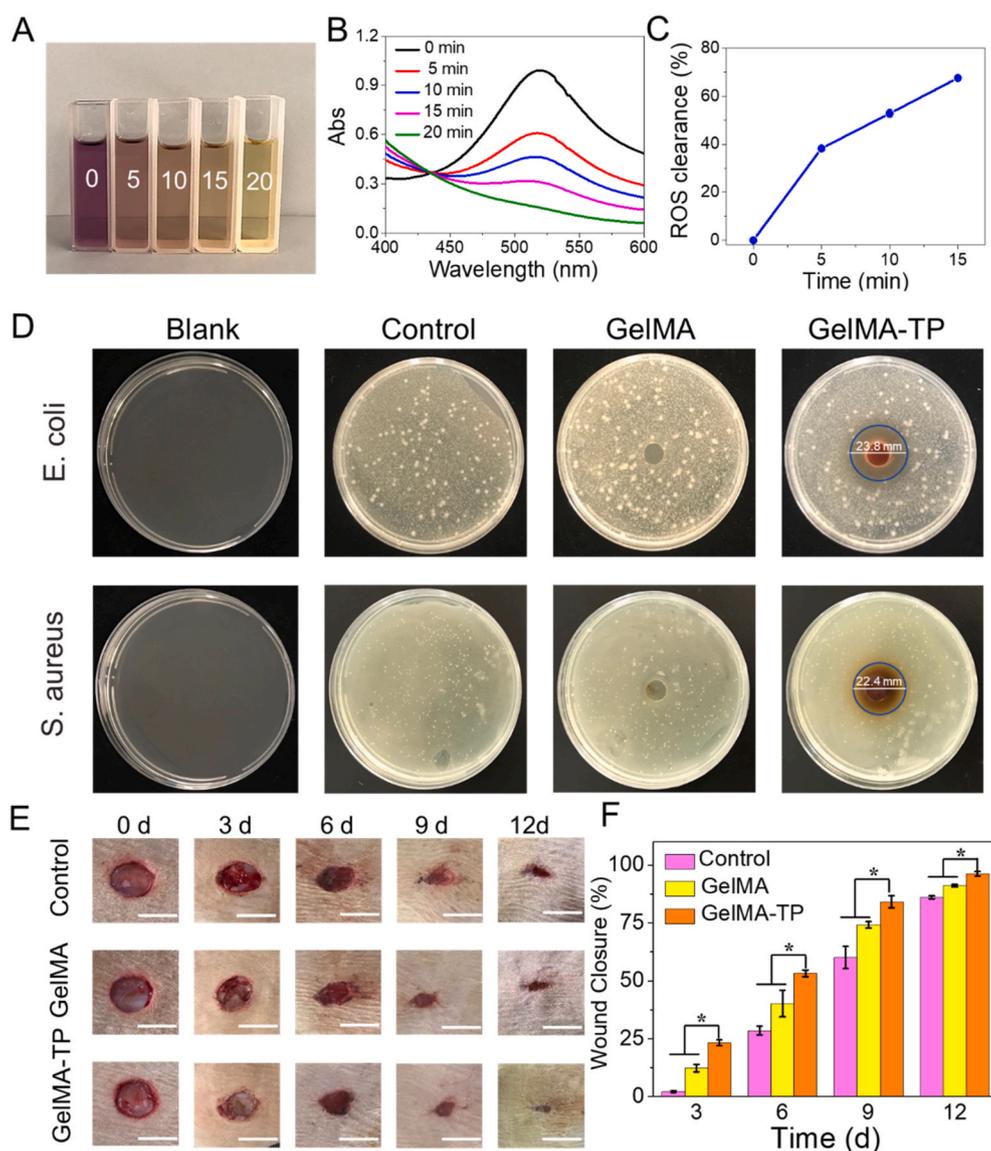
Fig. 6. A) Photographs of GelMA-TP hydrogel treated DPPH solutions with the time ranging from 0 to 20 min. B) UV–vis absorption spectra of GelMA-TP hydrogel treated DPPH solutions with the time ranging from 0 to 20 min. C) DPPH clearance of GelMA-TP hydrogel versus time. D) Inhibition zones against *E. coli* and *S. aureus* of GelMA hydrogel and GelMA-TP hydrogel. E-F) In vivo wound healing evaluation, representative photographs of wound and wound closure rates after various treatments at days 0, 3, 6, 9, and 12. (Scale bar: 10 mm * indicates significance, *p < 0.05).

diameter of inhibition zone was around 23.8 mm) and *S. aureus* (the diameter of inhibition zone was around 22.4 mm), while no antibacterial loop appears in the blank group and pristine GelMA hydrogel in terms of inhibition zone method. In addition, flat colony counting method reveals that bacteria spread fully inside the culture dishes of control and GelMA groups. By contrast, the GelMA-TP group can completely inhibit the growth of both *E. coli* and *S. aureus* (Fig. S11). The above results indicate that TP truly affords an antibacterial property. Compared with other natural polymer-based hydrogels, the GelMA-TP hydrogels have not only excellent mechanical properties, but also antibacterial activities (Table S1).

3.6. Biocompatibility, biodegradability and wound healing

In the following experiment, the effect of GelMA-TP hydrogel on wound healing was inspected. Prior to in vivo experiment, the cytotoxicity and biodegradability of the hydrogels were tested. Fig. S12 shows that the viability of cells treated with GelMA-TP-48h hydrogel leaching solution at different times can be maintained above 90%, which is higher than that of GelMA-TA hydrogel, further indicating that GelMA-TP hydrogel has better biocompatibility than GelMA-TA hydrogel. The GelMA-TP hydrogel was implanted in Sprague-Dawley (SD) rats

subcutaneously and the appearance was recorded at different intervals. As presented in Fig. S13, the GelMA-TP hydrogel is completely degraded at 49 days. Then, a full-thickness skin defect model was employed to assay the enhanced wound-healing ability of the GelMA-TP hydrogel. The wound closure treated by GelMA and GelMA-TP-48h hydrogels were traced at different time periods and the untreated skin defects were set as the control group (Fig. 6E). It is seen that after 3 days of treatment, the difference in wound size among the GelMA-TP-48h, GelMA group and the control group begins to appear. On the 12th day postimplantation, compared with the control group and the GelMA group, the wound in the GelMA-TP group is significantly closed, and its healing efficiency reaches 96%, while control group and GelMA group only have the healing rates of 86% and 91% respectively (Fig. 6F). The results indicate that the GelMA-TP hydrogel can accelerate wound closure and skin regeneration. H&E staining was performed on the targeted tissues on 12-day to further evaluate the wound healing (Fig. S14). The wound in the GelMA-TP group is covered by continuous epithelial tissue, showing the best skin maturation, such as dense epidermis, well-organized dermis and hair follicles as mature skin appendages. In contrast, the wound in the blank and GelMA group is covered by incomplete and thin epidermis. In addition, the GelMA-TP group has the least unmatured granulation tissue, evidencing the better wound healing

function of the GelMA-TP gel.

4. Conclusions

In summary, inspired by stiffening phenomenon of tea eggs, natural polymer (NP) hydrogels with high strength and toughness were prepared by a simply immersing the pristine hydrogels in tea polyphenols (TP). The TP treatment could lead to a tremendous enhancement in comprehensive properties of original NP hydrogel, primarily owing to the hydrogen bonding interaction of TP with NP chains. One beneficial change was that the TP-treated NP hydrogels could resume hydrophilicity resulting from TP release and accompanied water permeation, which also afforded antibacterial and antioxidant functions. We demonstrated that GelMA-TP hydrogel could facilitate wound healing. Remarkably, the TP-treated 3D printed pristine hydrogel scaffolds could achieve considerable increase in mechanical performance, showing an ability to resist different deformations, which will be able to boost the advance in developing robust and biocompatible bioinks that cannot be realized by current species.

CRediT authorship contribution statement

Tengling Wu: Investigation, Data curation, Methodology, Formal analysis, Writing - original draft. **Chunyan Cui:** Investigation, Data curation. **Chuanchuan Fan:** Software, Data curation. **Ziyang Xu:** Software, Data curation. **Yang Liu:** Investigation, Data curation. **Wenguang Liu:** Conceptualization, Formal analysis, Writing - review & editing.

Declaration of competing interest

The authors declare that they have no known competing financial interests or personal relationships that could have appeared to influence the work reported in this paper.

Acknowledgements

Appendix A. Supplementary data

Supplementary data to this article can be found online at https://doi.org/10.1016/j.bioactmat.2021.02.009.

References

[1] Z.T. Bao, C.H. Xian, Q.J. Yuan, G.T. Liu, J. Wu, Natural polymer-based hydrogels with enhanced mechanical performances: preparation, structure, and property, Adv. Healthcare Mater. 8 (2019) 1900670.

[2] S. Ladet, L. David, A. Domard, Multi-membrane hydrogels, Nature 452 (2008), 76-U6.

[3] J.M. Zuidema, M.M. Pap, D.B. Jaroch, F.A. Morrison, R.J. Gilbert, Fabrication and characterization of tunable polysaccharide hydrogel blends for neural repair, Acta Biomater. 7 (2011) 1634–1643.

[4] E. Sanmartín-Masiá, S. Poveda-Reyes, G.G. Ferrer, Extracellular matrix-inspired gelatin/hyaluronic acid injectable hydrogels, Int. J. Polym. Mater. Polym. Biomater. 66 (2016) 280–288.

[5] C.L. Liu, H.J. Zhang, X.Y. You, K.P. Cui, X.C. Wang, Electrically conductive tough gelatin hydrogel, Adv. Electron. Mater. 6 (2020), 2000040.

[6] W. Wang, Y.Y. Zhang, W.G. Liu, Bioinspired fabrication of high strength hydrogels from non-covalent interactions, Prog. Polym. Sci. 71 (2017) 1–25.

[7] Y.S. Zhang, A. Khademhosseini, Advances in engineering hydrogels, Science 356 (2017), eaaf3627.

[8] Z. Jiang, B. Diggle, I.C.G. Shackleford, L.A. Connal, Tough, self-healing hydrogels capable of ultrafast shape changing, Adv. Mater. 31 (2019), 1904956.

[9] H.C. Yu, S.Y. Zheng, L.T. Fang, Z.M. Ying, M. Du, J. Wang, K.F. Ren, Z.L. Wu, Q. Zheng, Reversibly transforming a highly swollen polyelectrolyte hydrogel to an extremely tough one and its application as a tubular grasper, Adv. Mater. 32 (2020), 2005171.

[10] T. Yuan, X.M. Cui, X.K. Liu, X.X. Qu, J.Q. Sun, Highly tough, stretchable, self-healing, and recyclable hydrogels reinforced by in situ-formed polyelectrolyte complex nanoparticles, Macromolecules 52 (2019) 3141–3149.

[11] B. Liu, Z.Y. Xu, H.J. Gao, C.C. Fan, G.S. Ma, D.F. Zhang, M. Xiao, B.J. Zhang, Y. Yang, C.Y. Cui, T.L. Wu, X.Q. Feng, W.G. Liu, Stiffness self-tuned shape memory hydrogels for embolization of aneurysm, Adv. Funct. Mater. 30 (2020), 1910197.

[12] J.Y. Sun, X.H. Zhao, W.R.K. Illeperuma, O. Chaudhuri, K.H. Oh, D.J. Mooney, J.J. Vlassak, Z.G. Suo, Highly stretchable and tough hydrogels, Nature 489 (2012) 133–136.

[13] H. Xue, Y.G. Tu, M. Xu, M.F. Liao, W.X. Luo, W.B. Guo, G.W. Zhang, Y. Zhao, Changes in physicochemical properties, gel structure and in vitro digestion of marinated egg white gel during braising, Food Chem. 330 (2020), 127321.

[14] H. Xue, M. Xu, M.F. Liao, W.X. Luo, G.W. Zhang, Y.G. Tu, Y. Zhao, Effects of tea and illicium verum braise on physicochemical characteristics, microstructure, and molecular structure of heat-induced egg white protein gel, Food Hydrocolloids 110 (2021), 106181.

[15] X.X. Zhou, T. Chen, H.H. Lin, H. Chen, J.H. Liu, F. Lyu, Y.T. Ding, Physicochemical properties and microstructure of surimi treated with egg white modified by tea polyphenols, Food Hydrocolloids 90 (2019) 82–89.

[16] Z.H. Chen, C.H. Wang, J.Z. Chen, X.D. Li, Biocompatible, functional spheres based on oxidative coupling assembly of green tea polyphenols, J. Am. Chem. Soc. 135 (2013) 4179–4182.

[17] D. Pasrija, C. Anandharamakrishnan, Techniques for extraction of green tea polyphenols: a review, Food Bioprocess Technol. 8 (2015) 935–950.

[18] B.C. Liu, Y. Wang, Y. Miao, X.Y. Zhang, Z.X. Fan, G. Singh, X.Y. Zhang, K. Xu, B.Y. Li, Z.Q. Hu, M. Xing, Hydrogen bonds autonomously powered gelatin methacrylate hydrogels with super-elasticity, self-heal and underwater self-adhesion for sutureless skin and stomach surgery and E-skin, Biomaterials 171 (2018) 83–96.

[19] H.L. Fan, J.H. Wang, Z.X. Jin, Tough, swelling-resistant, self-healing, and adhesive dual-cross-linked hydrogels based on polymer-tannic acid multiple hydrogen bonds, Macromolecules 51 (2018) 1696–1705.

[20] G.R. Cameron, R.F. Milton, J.W. Allen, Lancet, Toxicity of tannic acid 2 (1943) 179–186.

[21] W.C. Wilson, A.R. Macgregor, C.P. Stewart, The clinical course and pathology of burns and scalds under modern methods of treatment, Br. J. Surg. 25 (1938) 826–865, 1938.

[22] Z.H. Guo, Y. Yang, Y. Shu, L. Qiao, M. Peng, Z.P. Wang, Stimulus-responsive tea polyphenols as nanocarrier for selective intracellular drug delivery, J. Biomater. Appl. 35 (2020) 149–157.

[23] S. Saric, M. Notay, R.K. Sivamani, Green tea and other tea polyphenols: effects on sebum production and acne vulgaris, Antioxidants 6 (2017) 2.

[24] H. Yamada, H. Watanabe, Tea polyphenols in preventing cardiovascular diseases, Cardiovasc. Res. 73 (2007) 439–440.

[25] M. Saito, K. Saito, N. Kunisaki, S. Kimura, Green tea polyphenols inhibit metalloproteinase activities in the skin, muscle, and blood of rainbow trout, J. Agric. Food Chem. 50 (2002) 7169–7174.

[26] R. Amarowicz, R.B. Pegg, D.A. Bautista, Antibacterial activity of green tea polyphenols against Escherichia coli K 12, Nahrung 44 (2000) 60–62.

[27] K. Maji, S. Dasgupta, R. Bhaskar, M.K. Gupta, Photo-crosslinked alginate nano-hydroxyapatite paste for bone tissue engineering, Biomed. Mater. 15 (2020), 055019.

[28] N. Han, Z.Y. Xu, C.Y. Cui, Y. Li, D.F. Zhang, M. Xiao, C.C. Fan, T.L. Wu, J.H. Yang, W.G. Liu, A Fe^{3+}-crosslinked pyrogallol-tethered gelatin adhesive hydrogel with antibacterial activity for wound healing, Biomater. Sci. 8 (2020) 3164–3172.

[29] T.L. Wu, C.Y. Cui, Y.T. Huang, Y. Liu, C.C. Fan, X.X. Han, Y. Yang, Z.Y. Xu, B. Liu, G.W. Fan, W.G. Liu, Coadministration of an adhesive conductive hydrogel patch and an injectable hydrogel to treat myocardial infarction, ACS Appl. Mater. Interfaces 12 (2020) 2039–2048.

[30] T.L. Wu, Z.Y. Xu, Y.Y. Zhang, H.B. Wang, C.Y. Cui, B.G. Chang, X.Q. Feng, W.G. Liu, A pH-responsive biodegradable high-strength hydrogel as potential gastric resident filler, Macromol. Mater. Eng. 303 (2018), 1800290.

[31] J. Liang, F. Li, Y. Fang, W.J. Yang, X.X. An, L.Y. Zhao, Z.H. Xin, L. Cao, Q.H. Hu, Synthesis, characterization and cytotoxicity studies of chitosan-coated tea polyphenols nanoparticles, Colloids Surf., B 82 (2011) 297–301.

[32] M. Rizwan, G.S.L. Peh, H.-P. Ang, N.C. Lwin, K. Adnan, J.S. Mehta, W.S. Tan, E.K.F. Yim, Sequentially-crosslinked bioactive hydrogels as nano-patterned substrates with customizable stiffness and degradation for corneal tissue engineering applications, Biomaterials 120 (2017) 139–154.

[33] K. Lei, K.Q. Wang, Y.L. Sun, Z. Zheng, X.L. Wang, Rapid-fabricated and recoverable dual-network hydrogel with inherently anti-bacterial abilities for potential adhesive dressings, Adv. Funct. Mater. (2020), 2008010.

[34] H. Yamada, H. Watanabe, Tea polyphenols in preventing cardiovascular diseases, Cardiovasc. Res. 73 (2007) 439–440.